CHAPTER IV

RESULTS AND DISCUSSION

4.1 Microcapsule Size and Particle Size Distribution

4.1.1 Mean Particle Size

4.1.1.1 Dependence of Mean Particle Size on Homomixing Time

An organic-water emulsion was stirred strongly by 9000 rpm at room temperature for 4 min by a homomixer. The changes in particle size of microcapsules prepared from the different diisocyantes, HDI and MDI, and concentrations were investigated and illustrated in Figure 4.1.

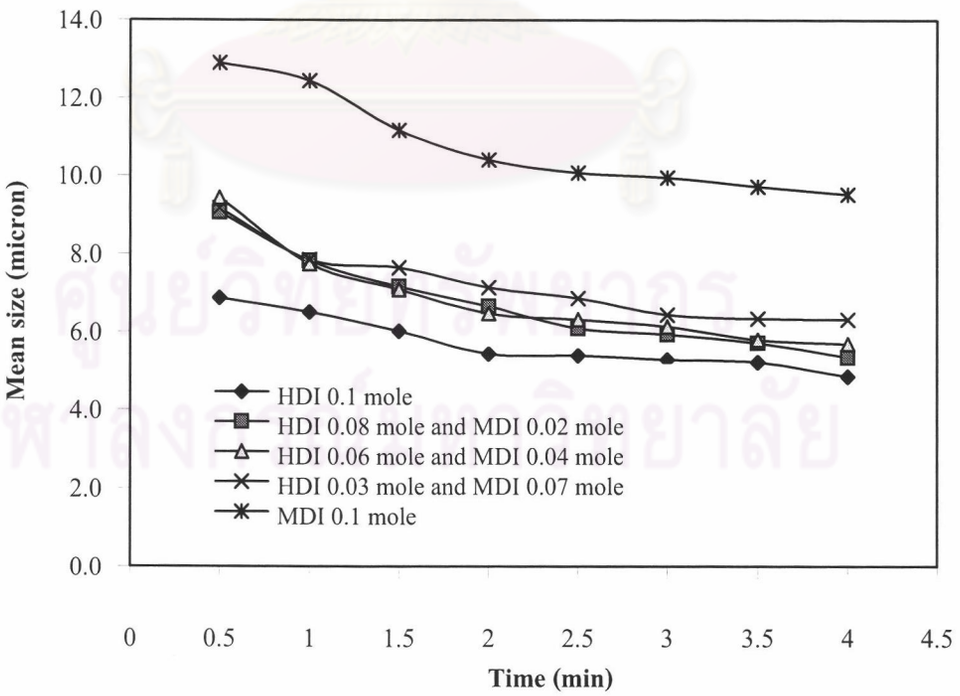

Figure 4.1 Mean particle size of polyurea microcapsules in various homomixing times.

As shown in Figure 4.1, mean particle size of all formulations had drastic changes in the time interval at the start to 2 min and a slow change from 2- 4 min. The mean size of microcapsules from HDI in the mixture shifted to the smaller sizes. The increase in size is imposed by the increased MDI ratio due to the rapid wall-forming, while the HDI/MDI- based microcapsules had a relatively small size.

4.1.1.2 Mean Particle Size at 4 min of Homomixing

Table 4.1 shows the particle size and particle sized distribution attained at 4 min. The mean particle size of each formulation was shown in Table 4.1. Mean particle size of HDI-based microcapsules was in the range of 3.6-3.8 micrometers while 6.2-6.9 micrometers for MDI-based microcapsules; HDI/MDI-based microcapsules was of relatively small size, 4.0-4.7 micrometers. The amount of wall material had no effect to the mean particle size.

Table 4.1 Particle size distribution and mean particle.

Formulation (HDI/MDI)	**Particle Size (μm)**			**Mean Particle (μm)**
	25% Distribution	50% Distribution	75% Distribution	
1 (0.10/0.00)	2.236	4.851	7.338	3.857
2 (0.08/0.02)	2.541	5.343	8.103	4.250
3 (0.06/0.04)	2.863	5.685	8.260	4.478
4 (0.03/0.07)	3.288	6.341	8.808	4.792
5 (0.00/0.10)	5.565	8.368	10.765	6.927
6 (0.07/0.00)	2.098	4.601	6.758	3.538
7 (0.06/0.01)	2.090	4.574	6.727	3.544
8 (0.04/0.03)	3.447	6.338	8.944	4.993

Table 4.1 Continued particle size distribution and mean particle.

Formulation (HDI/MDI)	Particle Size (μm)			Mean Particle (μm)
	25% Distribution	50% Distribution	75% Distribution	
9 (0.02/0.05)	3.030	5.687	7.918	4.414
10 (0.00/0.07)	5.107	7.913	10.413	6.609
11 (0.00/0.05)	2.160	4.707	7.062	3.694
12 (0.04/0.01)	2.418	4.964	7.373	3.933
13 (0.03/0.02)	2.677	5.435	7.809	4.199
14 (0.02/0.03)	2.691	5.453	7.513	4.050
15 (0.00/0.05)	4.768	7.543	9.970	6.271

4.1.2 Particle Size Distribution

Figure 4.2 shows the particle size distribution of polyurea microcapsules from the different diisocyanates and concentrations. The particle size distribution data was shown in Table 4.1. MDI-based polyurea microcapsules had a wider particle size distribution than HDI alone and HDI-MDI based microcapsules. The size distribution becomes wider with the increase of MDI, which is related to high reactivity of the emulsion globules of microcapsules containing MDI. The MDI-based microcapsules obtained in the early stage of homo mixing had thus a more random size of emulsion globules. The particle size distribution of the microcapsules from different amounts of wall materials, 0.07 and 0.05 mole, had the same typical size distribution as showed in Figures A.3-A.7.

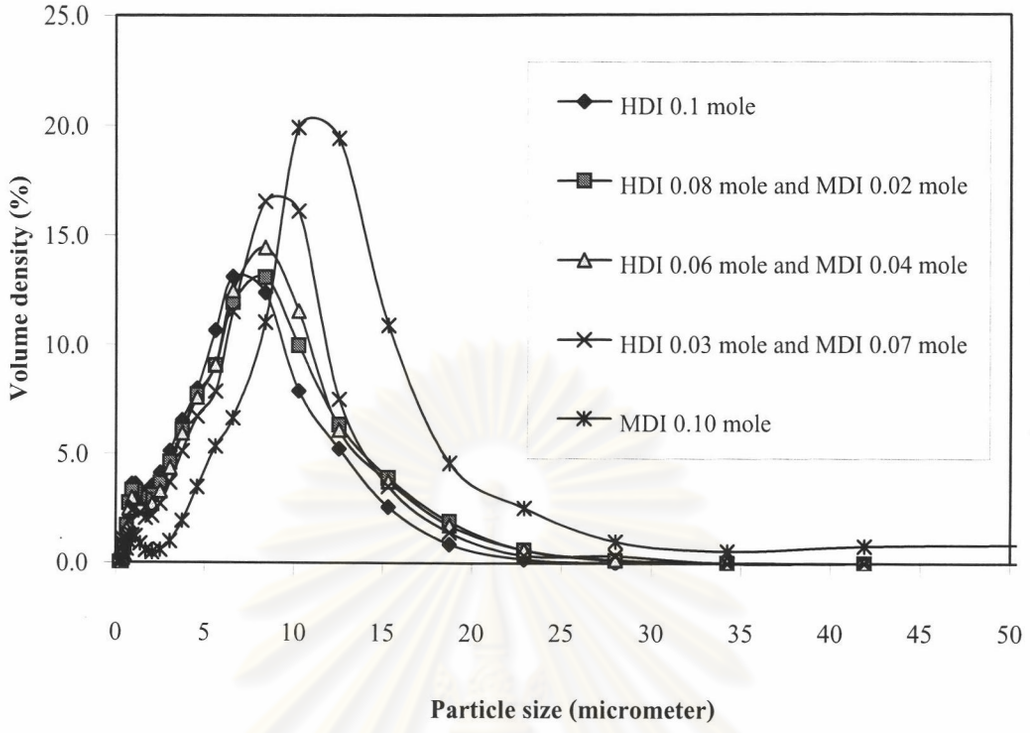

Figure 4.2. %Volume density of polyurea microcapsules prepared by 0.1 mole of different ratio of HDI and MDI.

4.2 Characterization of Polyurea Microcapsules

4.2.1 FTIR

Polyurea wall was obtained from the reaction between water and diisocyanates, HDI and MDI. A reaction temperature of 85-90°C was used and maintained for 5 hours. The chemical reactions of HDI and MDI were presented as follows:

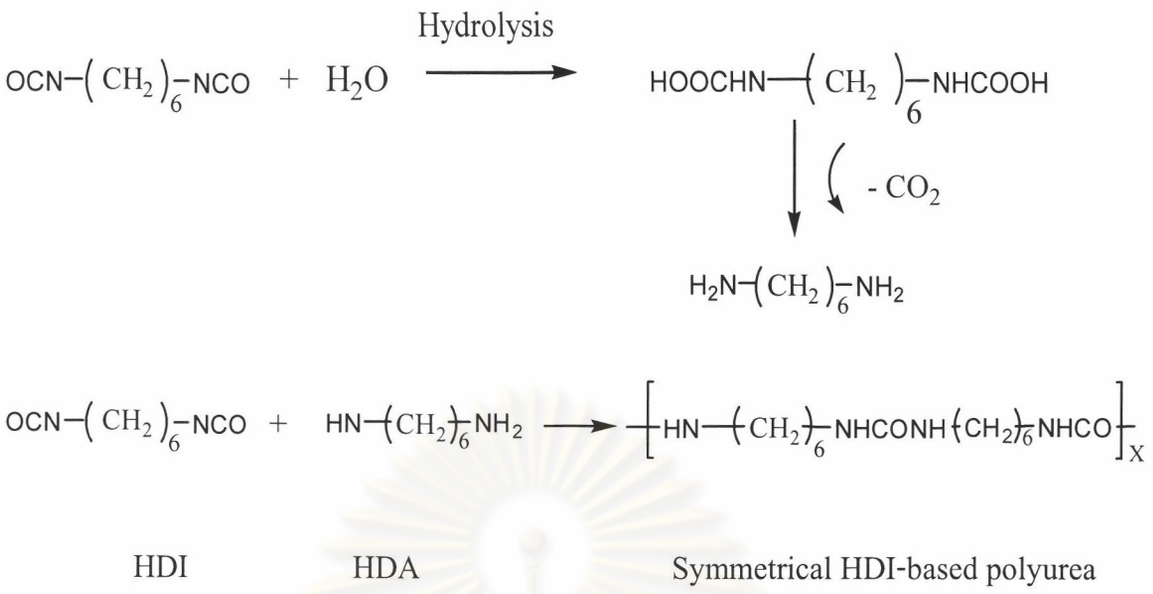

Scheme 4.1 The formation of polyurea wall from HDI.

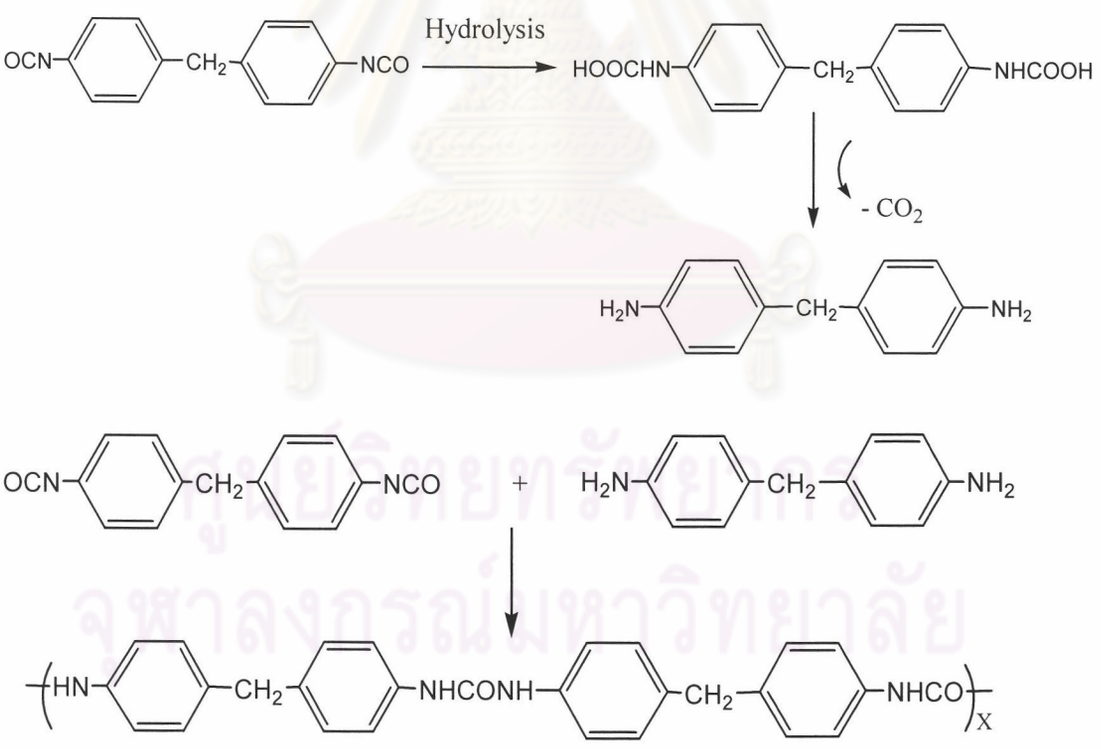

Symmetrical MDI-based polyurea

Scheme 4.2 The formation of polyurea wall from MDI.

In the presence of EDA, the reactions between EDA and diisocyanate of both MDI and HDI were presented as follows:

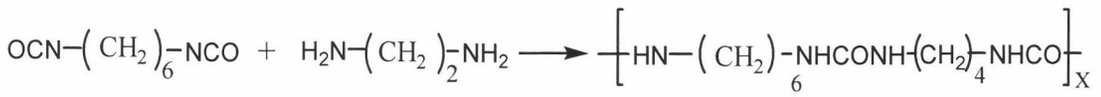

Asymmetrical HDI-based Polyurea

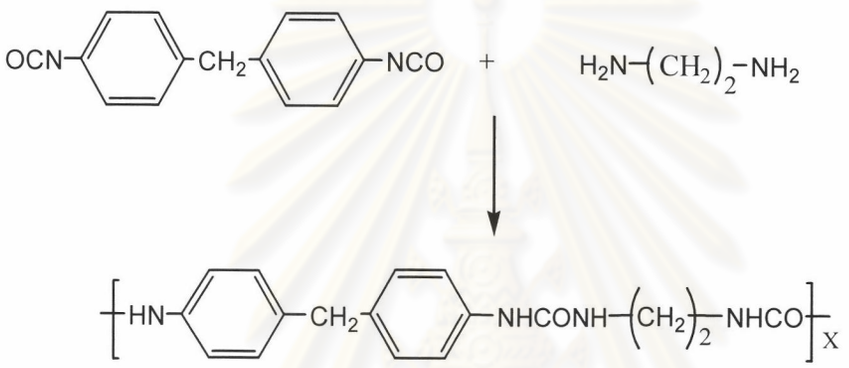

Asymmetrical MDI-based Polyurea

Scheme 4.3 The formation of polyurea wall from the reaction between EDA and diisocyanate.

The molecular structure was also confirmed by the FTIR spectra. The FTIR spectra of polyurea microcapsules are provided in Figures A8-A20. The spectrum shows the N-H absorption band at 3330-3360 cm^{-1} and C=0 absorption band at 1630 cm^{-1} and disappearance of NCO absorption bands at 2275 cm^{-1}. The C-H stretching in the HDI and EDA was observed at 2900 cm^{-1} and at 3000 cm^{-1} for MDI-based microcapsules. The C=C ring stretching of aromatic was observed at 1600 cm^{-1} and 1475 cm^{-1} for MDI-based polyurea microcapsules.

4.2.2 Scanning Electron Microscope (SEM)

4.2.2.1 Effect of Core-to-Wall Ratio

One of the most important parameters regarding microcapsules production is the relationship between wall thickness and diameter. Microcapsules can be single capsule or grouped together, unlike a bunch of grapes. This is extremely important, as it is directly related to the amount of raw materials consumed to produce the microcapsule wall, as well as to the performance and breakage stability of the microcapsules.[15]

In the interfacial polymerization process, the wall thickness [t] of the capsules in a single capsule emulsion is dependent on the quantities of wall material [A_w] (in our research, they are diisocyanate and ethylene diamine), core material [A_c] (the color former solution) used, and on the capsule diameter [d].

$$t = 1/2[((A_w/A_c)+1)^{1/3} - 1] (d-2t) \quad (4.1)$$

When t is much smaller than d, the ratio of wall thickness to diameter depends with sufficient accuracy only on the ratio of the amount of wall material to amount of core material. As the same ratio applies for all capsules (large or small) in a given microcapsule emulsion, it follows that for all capsules in an emulsion produced by interfacial polymerization process, the ratio of wall thickness to diameter remains constant. Based on the above-mentioned equation (eq. 4.1), one important parameter is the ratio of amount of wall material to the amount of core material according to the following statements:

- The wall thickness is directly proportional to the amount of wall material (HDI, MDI and EDA).

- The wall thickness is indirectly proportional to the amount of core material (solvent and CVL).

Morphologies of the microcapsules attained from 0.1, 0.08 or 0.05 mole of the wall material ratio (100:0, 80:20, 60:40, 30:70 and 0:100) are presented in Figures 4.3-4.8 and A.21-A.29. As seen from the Figure 4.3, wall material concentration of 0.05 mole had the incomplete spheres because the thinner wall and wall materials were not enough to form the microcapsule wall.

4.2.2.2 Effect of Diisocyanate

SEM micrographs of polyurea microcapsules from the different 0.10 molar ratios of HDI and MDI are demonstrated in Figures 4.4-4.8. The surface of the microcapsules from MDI alone became rougher and soft with some dented surface than the others. This was mainly due to the types of diisocyanate whose MDI, the aromatic diisocyanate, can be presented in the several resonances by the delocalization of negative charge, which can provide the superior reactivity of monomer. The reactivity of the monomer of the common isocyanates is compared in the Table B.4. It shows the reactivity of MDI is around 80 times higher than HDI. On the other hand, because of slow wall-formation by inferior reaction of HDI, microcapsules from HDI showed a bunch of capsules. (Figures 4.3, A.21 and A.26)

Figure 4.9 shows the SEM micrograph of micorcapsules after freezing and under pressure of 75 kg/cm^2. It shows that the surface of HDI-based microcapsules was rigid and fragile while the HDI-MDI and MDI alone based microcapsule were flexible. It seems to relate with the higher stiffness of HDI-based polyurea microcapsules. Due to a long chain linear structure, the polar group favors the development of a high crystalline structure.

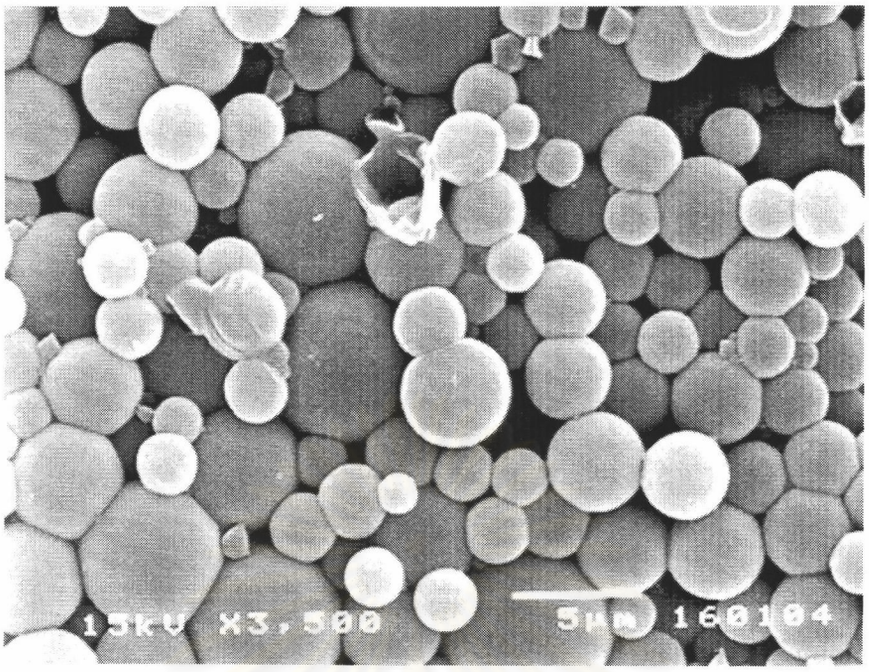

(a)

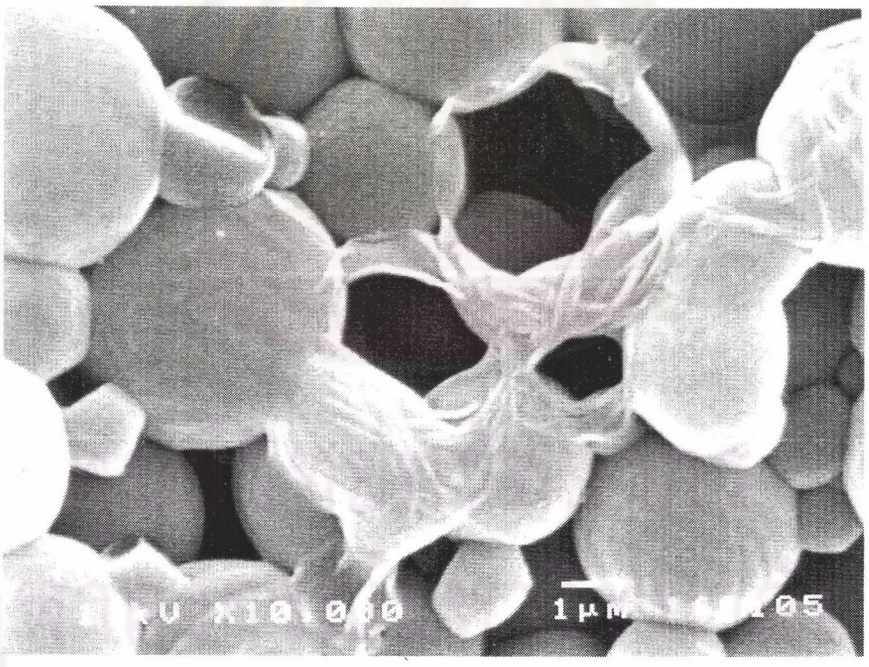

(b)

Figure 4.3 Scanning electron micrographs of polyurea microcapsules formulation 14: 0.02 mole HDI and 0.03 mole MDI in (a) and (b) with different magnifications.

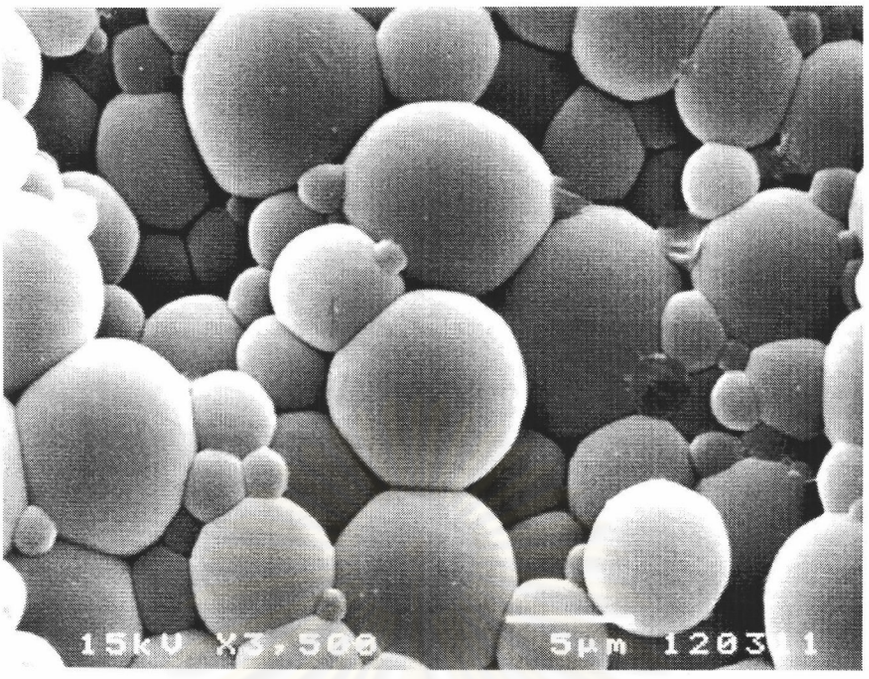

(a)

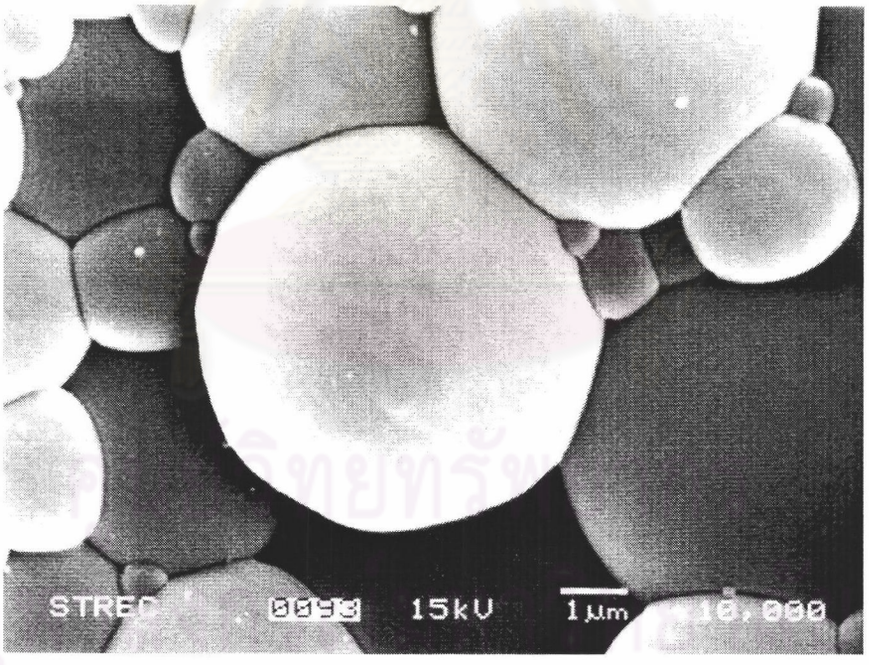

(b)

Figure 4.4 Scanning electron micrographs of polyurea microcapsules formulation 1: 0.10 mole HDI in (a) and (b) with different magnifications.

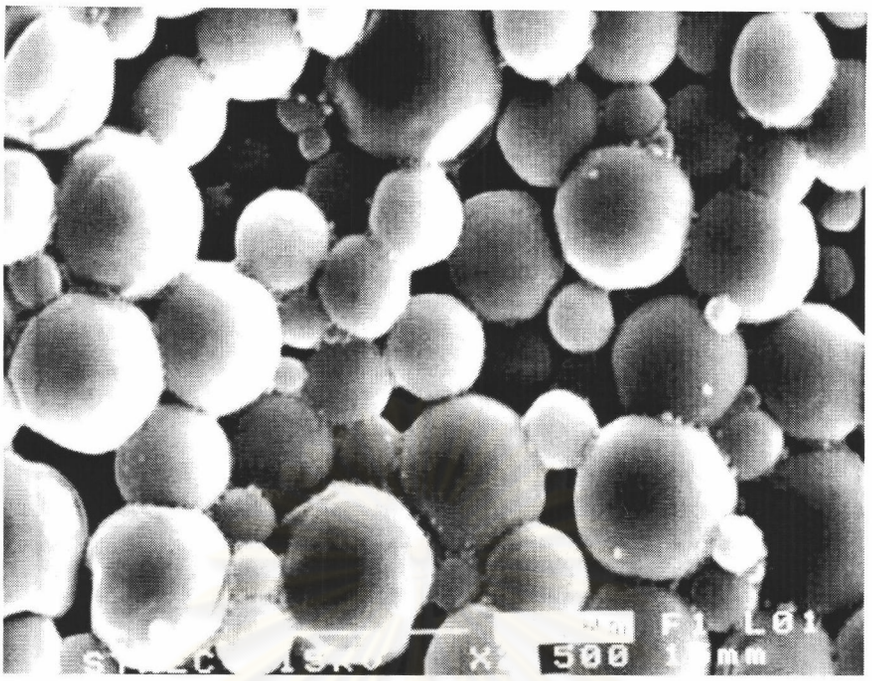

(a)

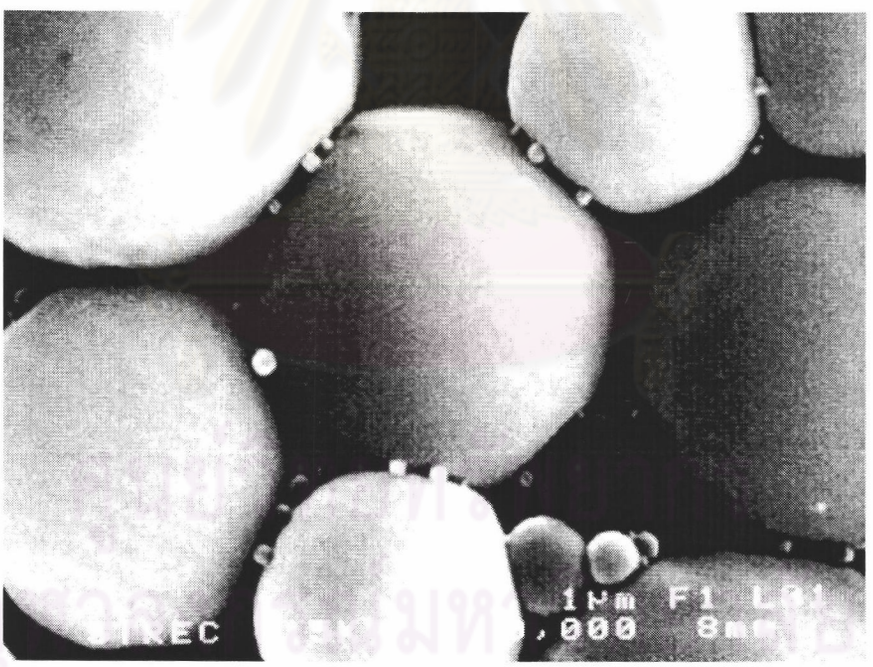

(b)

Figure 4.5 Scanning electron micrograph of polyurea microcapsules formulation 2: 0.08 mole HDI and 0.02 mole MDI in (a) and (b) with different magnifications.

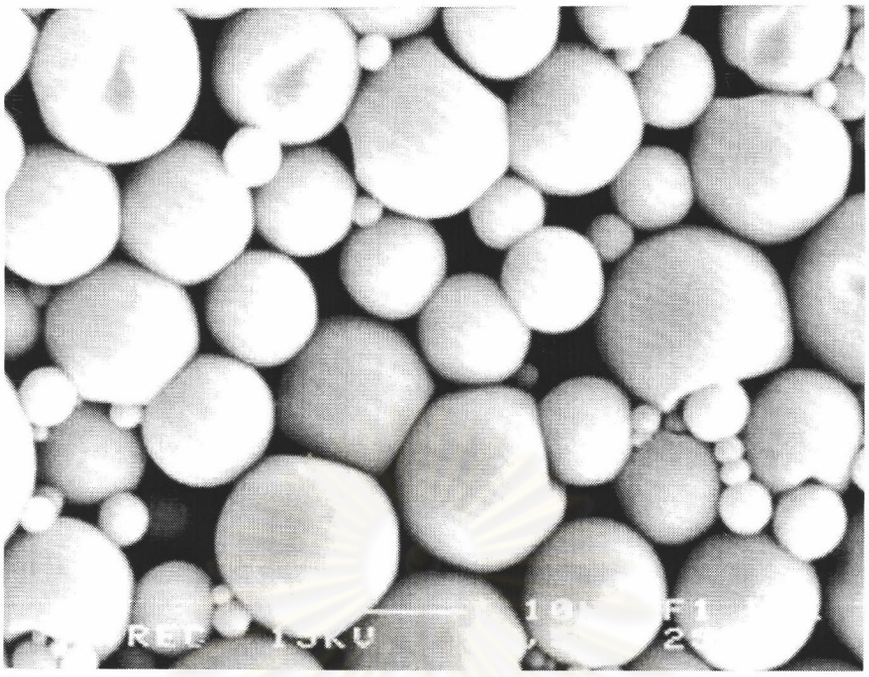

(a)

(b)

Figure 4.6 Scanning electron micrographs of polyurea microcapsules formulation 3: 0.06 mole HDI and 0.04 mole MDI in (a)and (b) with different magnifications.

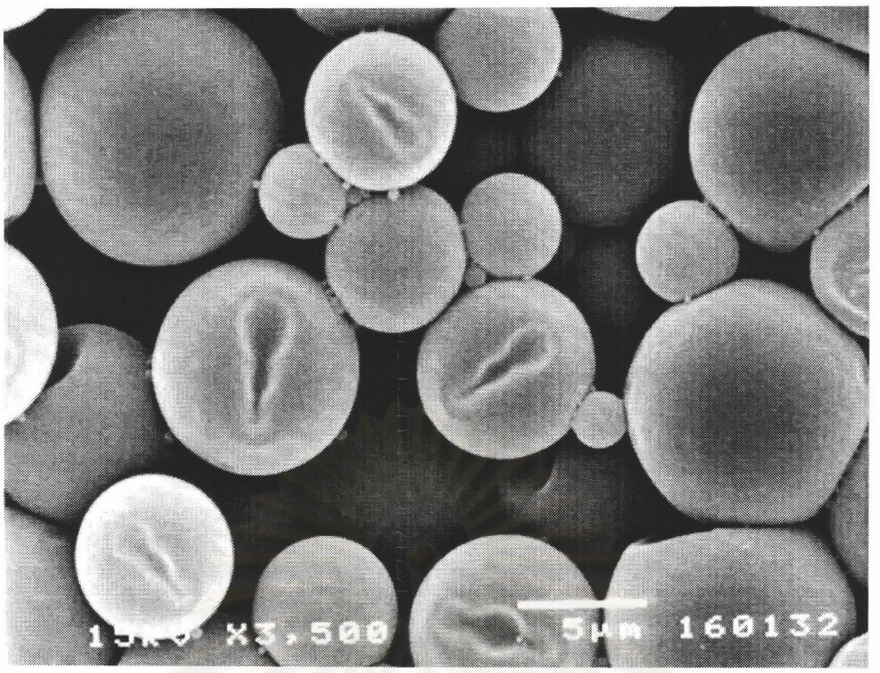

(a)

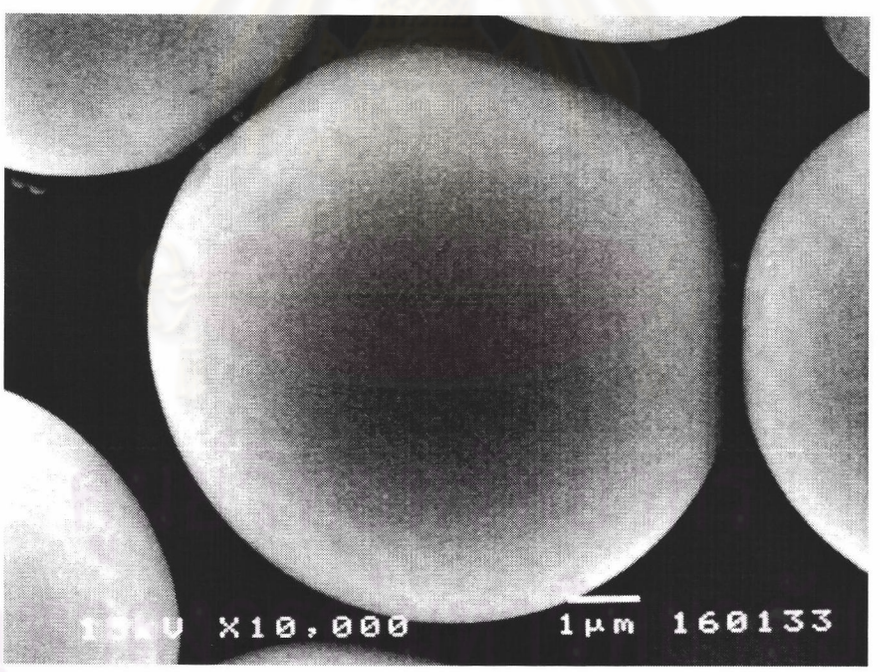

(b)

Figure 4.7 Scanning electron micrographs of polyurea microcapsules formulation 4: 0.03 mole HDI and 0.07 mole MDI in (a) and (b) with different magnifications.

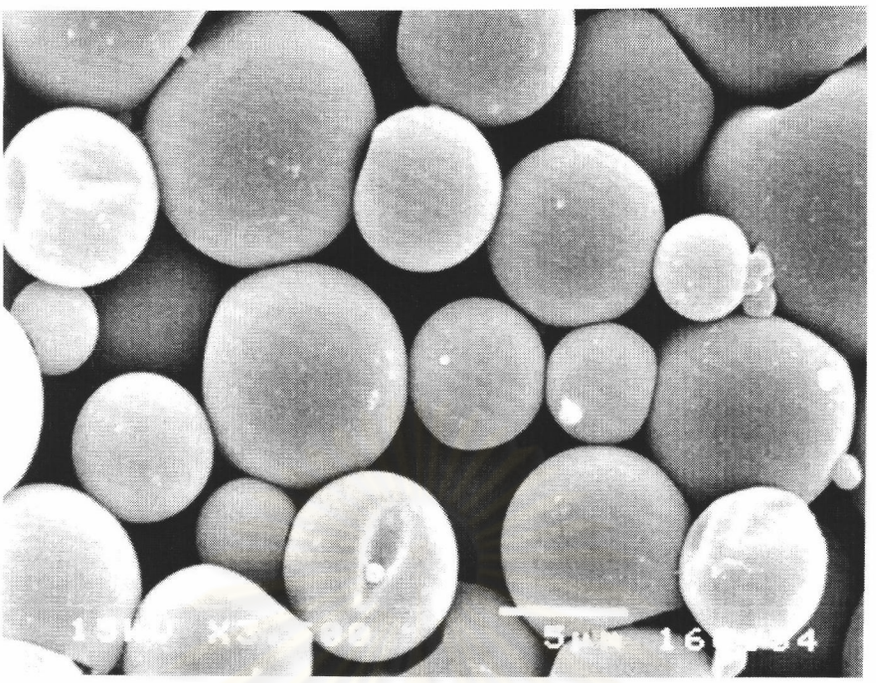

(a)

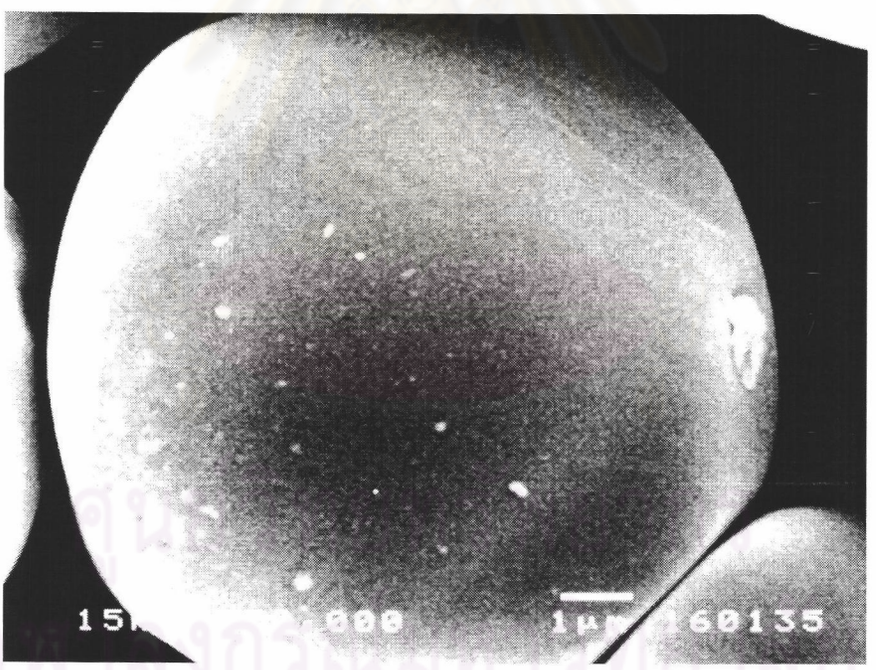

(b)

Figure 4.8 Scanning electron micrographs of polyurea microcapsules formulation 5: 0.1 mole MDI in (a) and (b) with different magnifications.

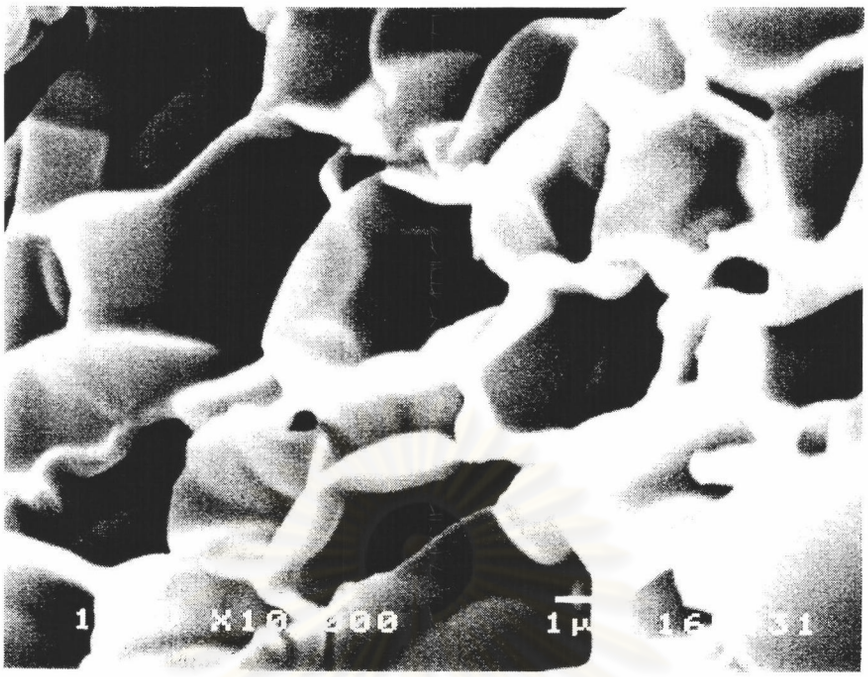

(a) Formulation 1: 0.10 mole HDI

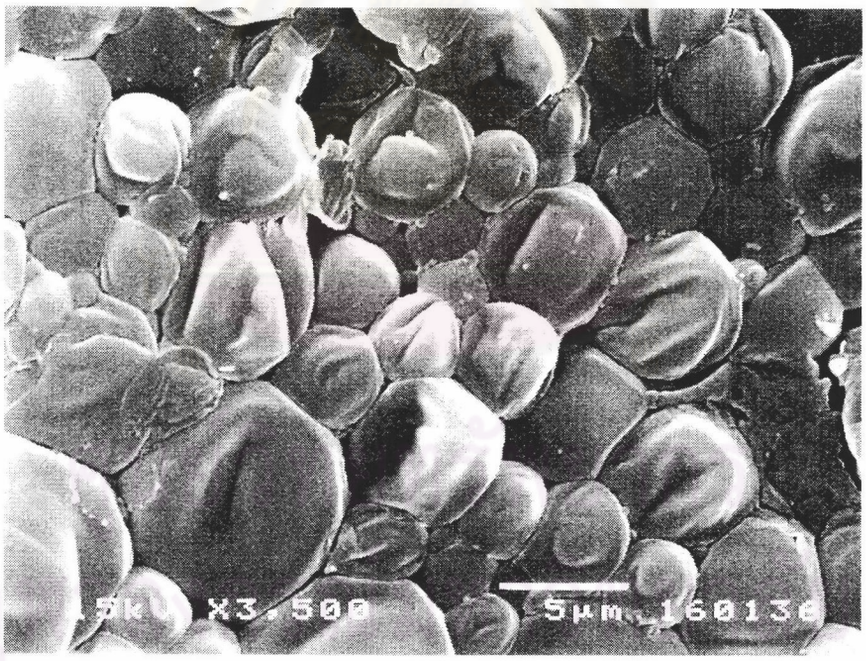

(b) Formulation 2: 0.08 mole HDI and 0.02 mole MDI

Figure 4.9 Scanning electron micrographs of polyurea microcapsules after freeze and under pressure 75 kg/cm^2.

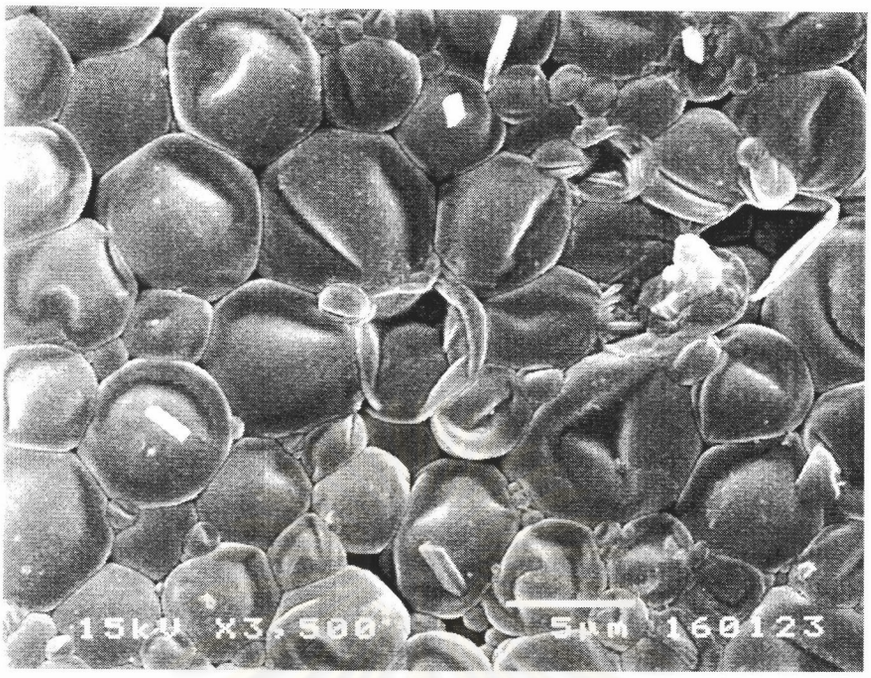

(c) Formulation 3: 0.06 mole HDI and 0.04 mole MDI

(d) Formulation 4: 0.03 mole HDI and 0.07 mole MDI.

Figure 4.9 Continued scanning electron micrographs of polyurea microcapsules after freeze and under pressure 75 kg/cm^2 (c) and (d).

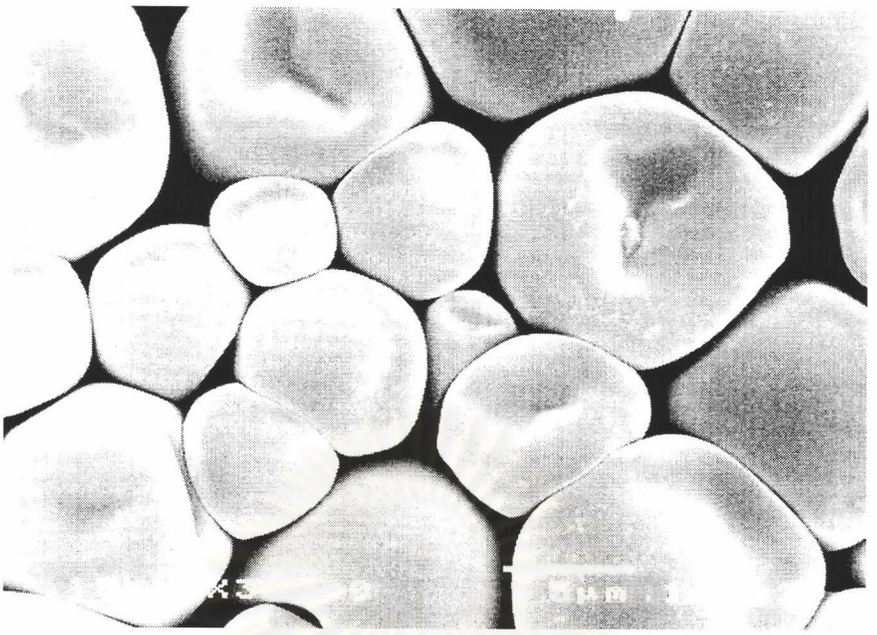

(e) Formulation 5: 0.10 mole MDI.

Figure 4.9 Continued scanning electron micrographs of polyurea microcapsules after freeze and under pressure 75 kg/cm^2 (e).

4.2.2.3 Effect of Ethylene Diamine (EDA)

Certain reactions other than the interfacial reaction can significantly affect the microencapsulation. Obviously, satisfactory microencapsulation cannot be expected when there is only a hydrolysis reaction of monomer to form the capsules. It is anticipated that an addition of EDA can also participate during the hydrolysis of diisocyanate. The morphologies of the microcapsules obtained from the different compositions differ as shown in Figures 4.10 to 4.12. As seen from these figures mentioned, the surface of microcapsules became rougher when EDA was added. Increases in the EDA concentration increase the roughness of the microcapsules. The reaction of EDA with diisocyanate is another contributor to the film properties. On the other hand, it depends on the type of diisocyanate as well as the amount of EDA added as shown in Figures A.30-A.35.

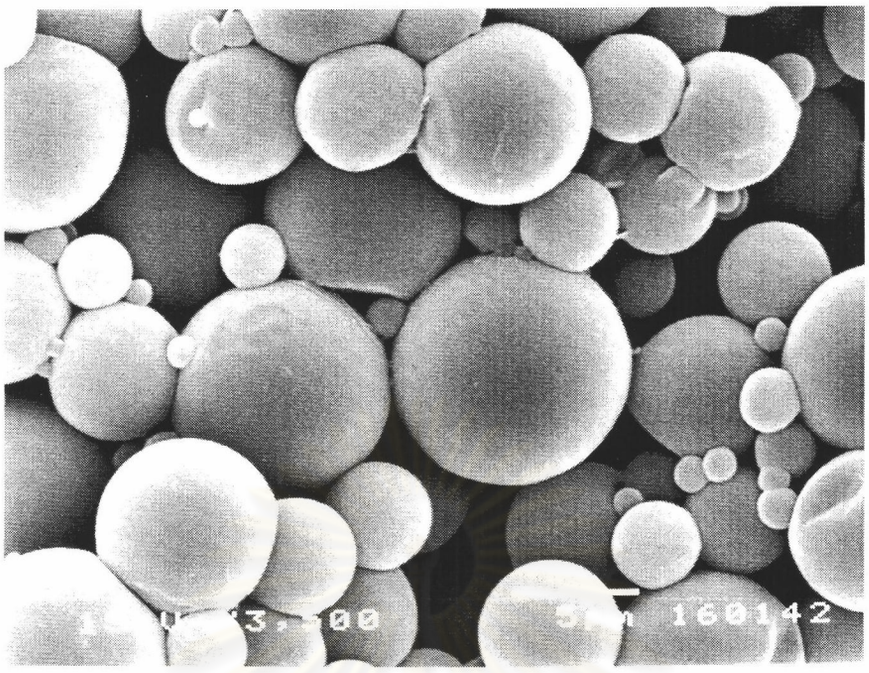

(a)

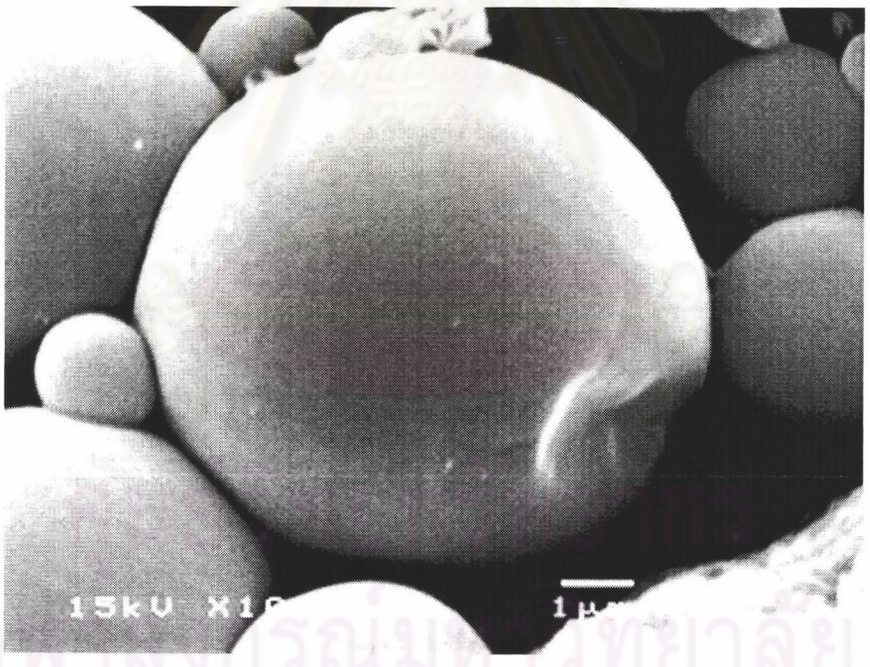

(b)

Figure 4.10 Scanning electron micrographs of polyurea microcapsules formulation 19: 0.06 mole HDI, 0.04 mole MDI and 0.01 mole EDA in (a) and (b) with different magnifications.

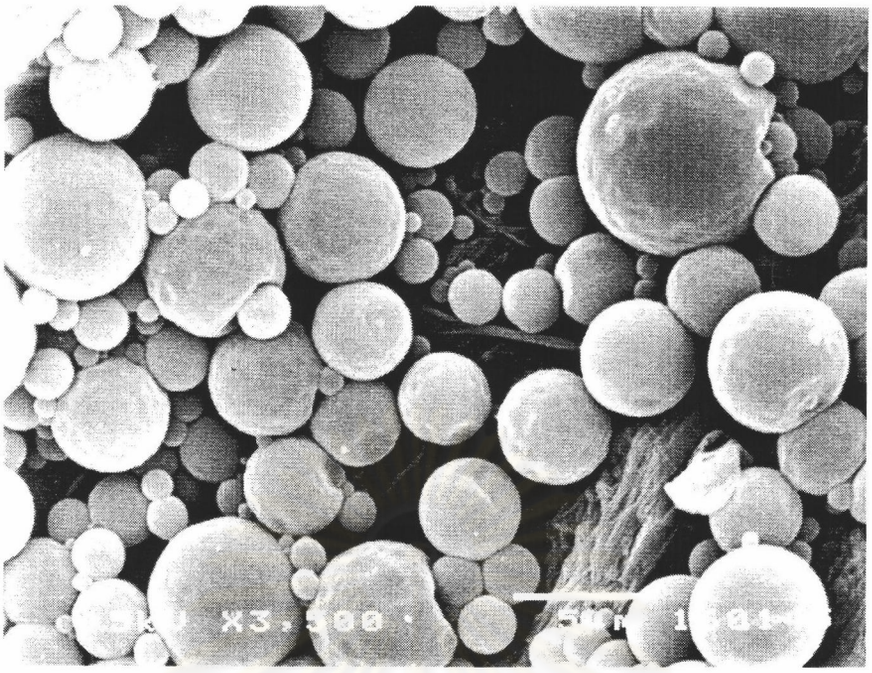

(a)

(b)

Figure 4.11 Scanning electron micrographs of polyurea microcapsules formulation 20 : 0.06 mole HDI, 0.04 mole MDI and 0.02 mole EDA in (a) and (b) with different magnifications.

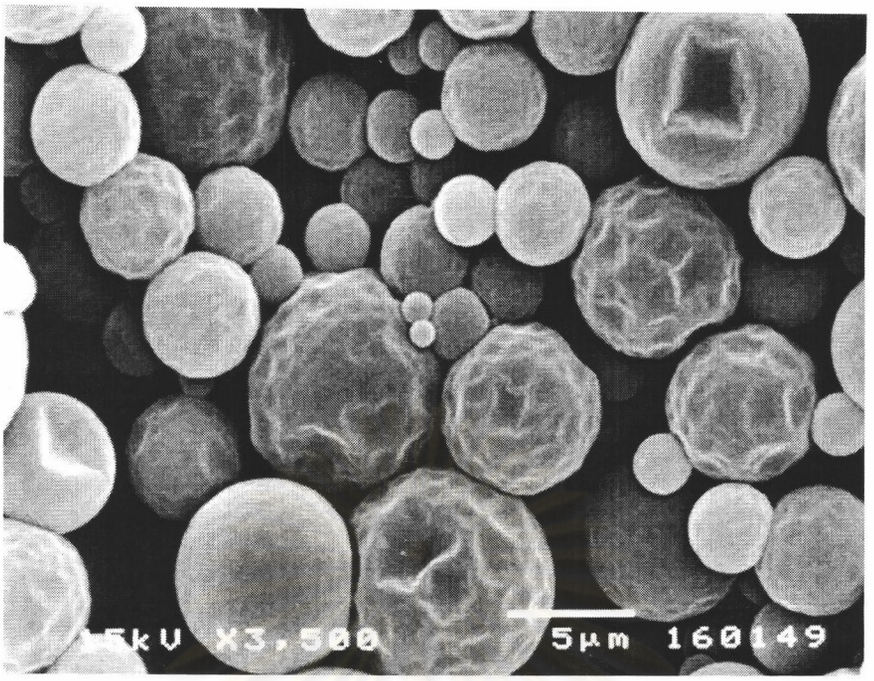

(a)

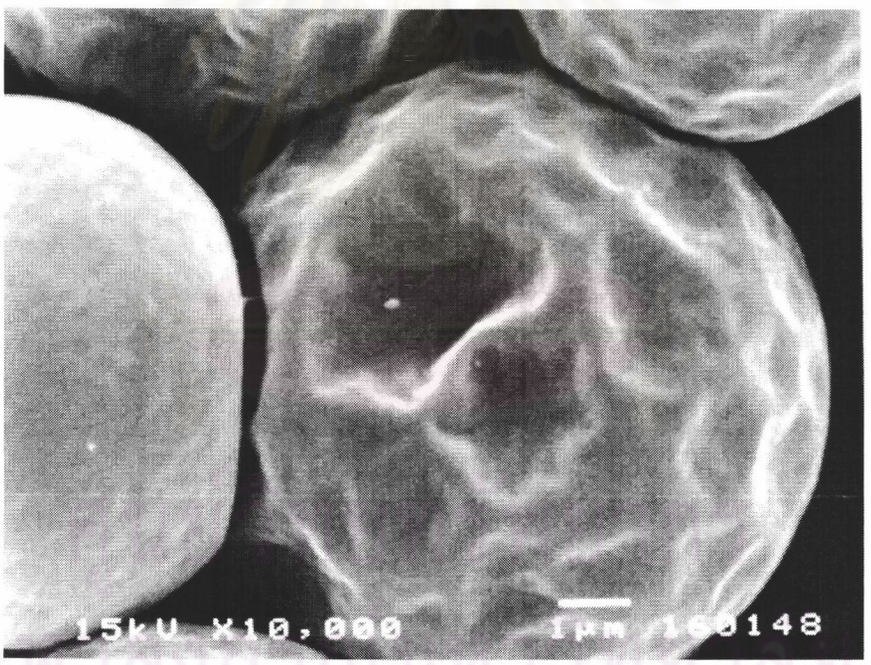

(b)

Figure 4.12 Scanning electron micrographs of polyurea microcapsules formulation 21: 0.06 mole HDI, 0.04 mole MDI and 0.03 mole EDA in (a) and (b) with different magnifications.

4.2.3 TGA

The microcapsules were investigated in a thermogravimetric with a heating rate of 10°C/min from 20-500°C under nitrogen atmosphere for analyzing their degradation behavior at elevated temperatures. All of the decomposition curves were shown in Figure 4.13. Figure A.36-A.40 showed the TGA curves of the polyurea microcapsule from different ratios of HDI and MDI. All the samples showed an initial weight loss from 170°C-270°C, of about 30% of the microcapsules from HDI only; 12% from MDI only and of about 20-28% from HDI-MDI based microcapsules. The subsequent weight loss, from 270°C-320°C, of up to 60% was found for the HDI-based microcapsules and 87% for the MDI-based microcapsules

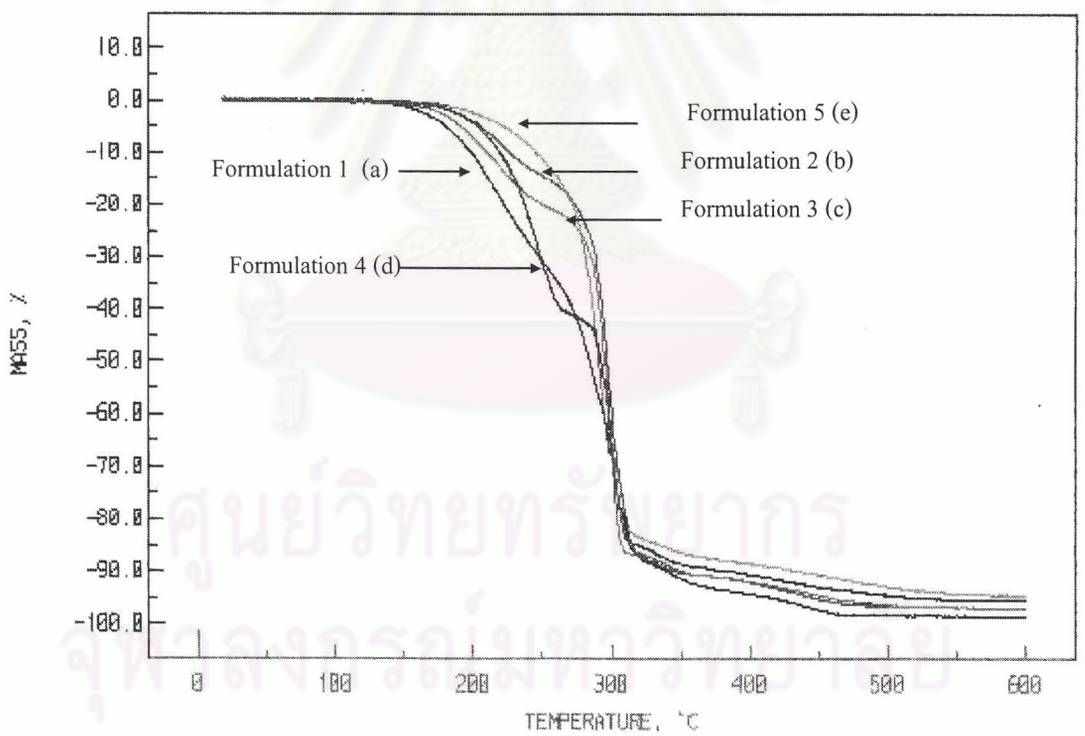

Figure 4.13 TGA thermograms of polyurea microcapsules from different mole ratio of diisocyanate of formulation 1 (a) 0.10 mole HDI, Formulation 2 (b) 0.08 mole HDI and 0.02 mole MDI, formulation 3 (c) 0.06 mole HDI and 0.04 mole MDI, formulation 4 (d) 0.03 mole HDI and 0.07 mole MDI, formulation 5 (e) 0.10 mole MDI.

Black residues were found into the samples containing MDI. The weight loss % of HDI and MDI–based microcapsules were relatively small whereas the weight loss of HDI only was comparatively large.

It is thus concluded that MDI microcapsules possessed better thermal stability than that of HDI-based microcapsules. Though MDI-based microcapsules showed the good thermal stability but they gave a blue color emulsion, which is caused by the premature reaction of leuco dye during the hydrolysis reaction. The optimal quality should be considered to achieve the purpose of manufacturer and requirements of end users.

4.3 Physical Appearance

The physical appearance of microcapsules emulsion was shown in Figure 4.14. As shown in this figure, the HDI-based microcapsules emulsion was white, the MDI-based emulsion gave blue color and the MDI alone emulsion gave deep blue color. Premature reaction caused by the leuco dye during the reaction produced the blue color.

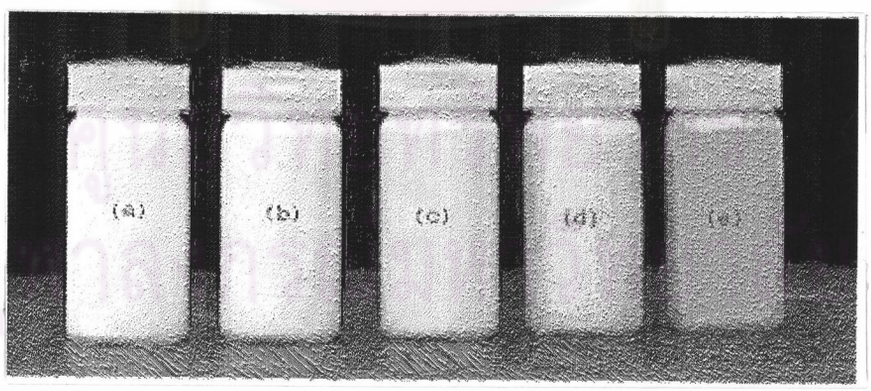

Figure 4.14 Physical appearance of the polyurea microcapsules from (a) 0.1 mole HDI, (b) 0.08 mole HDI and 0.02 mole MDI, (c) 0.06 mole HDI and 0.04 mole MDI, (d) 0.03 mole HDI and 0.07 mole MDI and (e) 0.10 mole MDI.

This phenomenon can be explained in the chemical reaction in Scheme 2.6. MDI and HDI were hydrolyzed by water. In this reaction, the primary product is the carbamic acid, which is not stable and will decompose to the corresponding amine and carbon dioxide. Though carbamic acid is unstable, but the rapid reaction of MDI with water can provide a strong acid enough to release proton or hydrogen ion. The phthalic anhydride linkage at the position of C-O- bond is thus cleaved, leading to a leveling out of the angular molecular structure and hence to the formation of the chromophore as shown in Scheme 4.4.

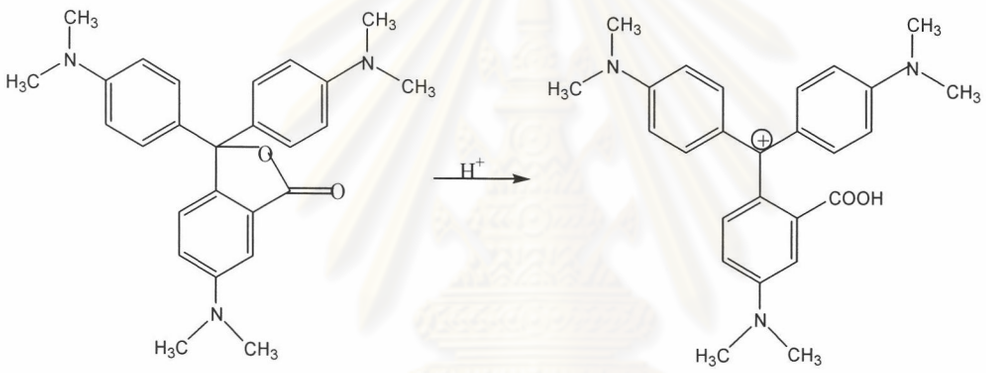

Colorless Dye Blue color former.

Scheme 4.4 The color developing of CVL.

4.4 Image Density

Image under pressure 20kg/cm^2 was developed and examined on the dye acceptor coating paper (CF) by a reflection densitometer. The results of the dominate color density was shown in Table 4.1. The effect of ethylene diamine (EDA) on the image density is pronounced depending on the contents of wall materials. This is related to lifespan of the wall stability, which keeps the core materials aside from being emulsified as a result of the unstable surface of the microcapsules.

Table 4.2 Image density

Formula No.	Mole Ratio HDI: MDI	EDA (mole)	Dominant color density (Cyan)
2	0.08:0.02	0.00	0.14
16		0.01	0.15
17		0.02	0.15
18		0.03	0.17
3	0.06:0.04	0.00	0.13
19		0.01	0.18
20		0.02	0.17
21		0.03	0.16
4	0.03:0.07	0.00	0.13
22		0.01	0.21
23		0.02	0.22
24		0.03	0.19

Core material: 9 g of CVL dissolved in 150 g of diisopropylnapthalene.

The MDI-based microcapsules needed less reaction time than HDI-base microcapsules due to the higher reactivity of MDI. Loss of the core material through the wall barely occurred during processing. Though the loading content of the core material of the MDI-based microcapsules is higher than that of the HDI, the image density was oppositely shown due to that the surface of the microcapsules became increasingly rougher with an increase of the MDI content. It is proposed that the addition of EDA determines the roughness level of the microcapsules. The results were obviously shown in the higher ratio of MDI. On the other hand, too high the EDA concentration yielded the thick microcapsule wall and the surface of the microcapsules

containing high EDA concentrations became rougher, which produced the lower density of image.[39]

4.5 Extent of Microencapsulation

4.5.1 Standard Curve of CVL

UV/Visible spectrophotometer was used to determine the encapsulated concentration of CVL in the microcapsules. In the aqueous solution, CVL can absorb UV light at the wavelength range of 352-353 nm. The wavelength used to analyze the neat (undeveloped) CVL in this study was 353 nm since it was the λ_{max} of the CVL in this medium. At this wavelength, there was no interference by other ingredients used to form the microcapsule wall and the vehicle had no significant absorption at 353 nm. Thus, the UV/Visible spectrophotometry technique could be used to assay the amount of CVL containing in the microcapsules.

Figure 4.15 shows the spectra of CVL standard solutions at various concentrations. A standard curve was plotted between the CVL absorbance at 353 nm. and its concentration. The curve was fitted using a linear regression analysis. The results are presented in Table 4.2 and Figure 4.16. A straight line is obtained with a coefficient of determination (r^2) of 0.9981. The regression equation of this line is

$$y = 0.005 + 0.0077x \qquad (4.2)$$

where y is the absorbance of CVL and x is the concentration of CVL solution in μg/ml. This equation was used to calculate the amount of CVL extracted from the microcapsules.

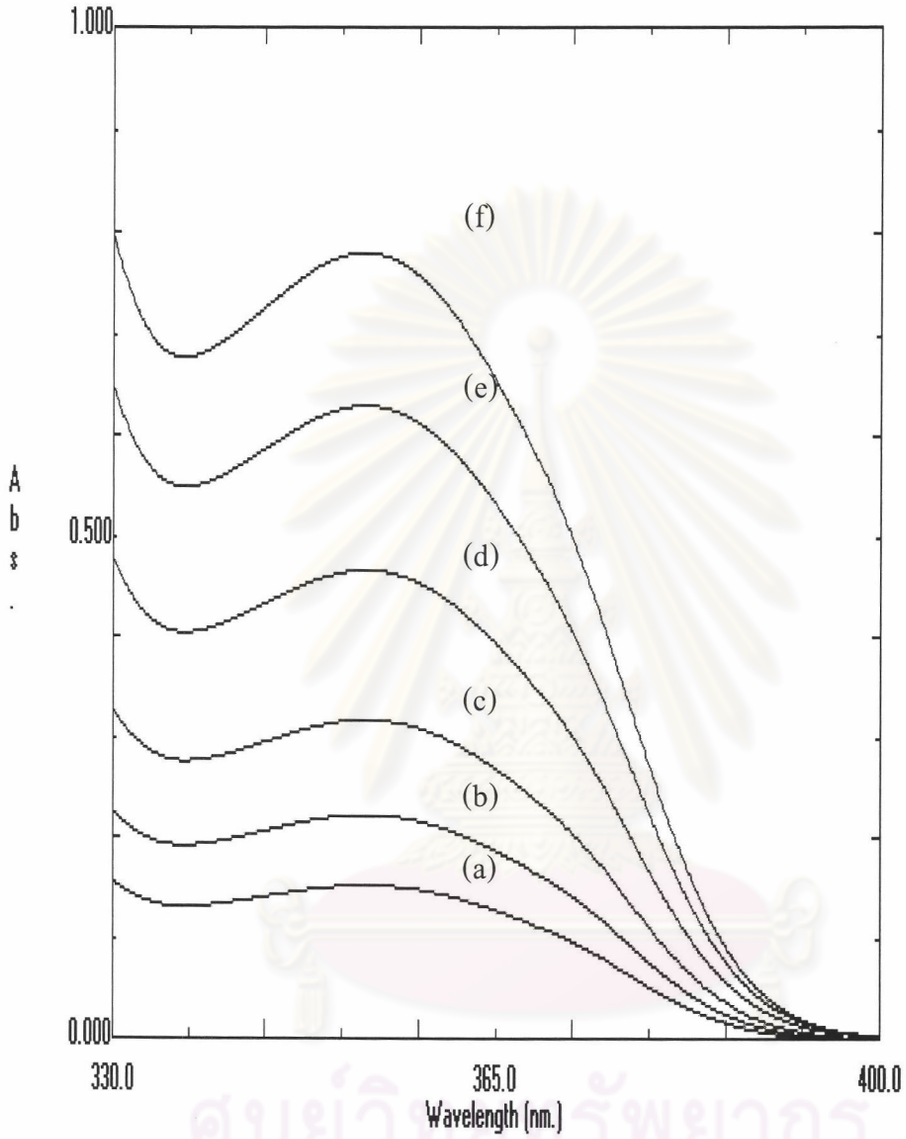

Figure 4.15 Absorbance of standard solutions of CVL at the concentrations of (a) 17.5, (b) 24.5, (c) 35.0, (d) 52.5, (e) 70.0 and (f) 87.5 μg/ml.

Table 4.3 Absorbance of the standard solutions of the CVL assayed by UV/Visible spectrophotometry.

Standard solution no.	Concentration (μg/ml)	Absorbance at 353 nm
1	17.50	0.157
2	24.50	0.226
3	35.00	0.339
4	52.50	0.478
5	70.00	0.626
6	87.50	0.806

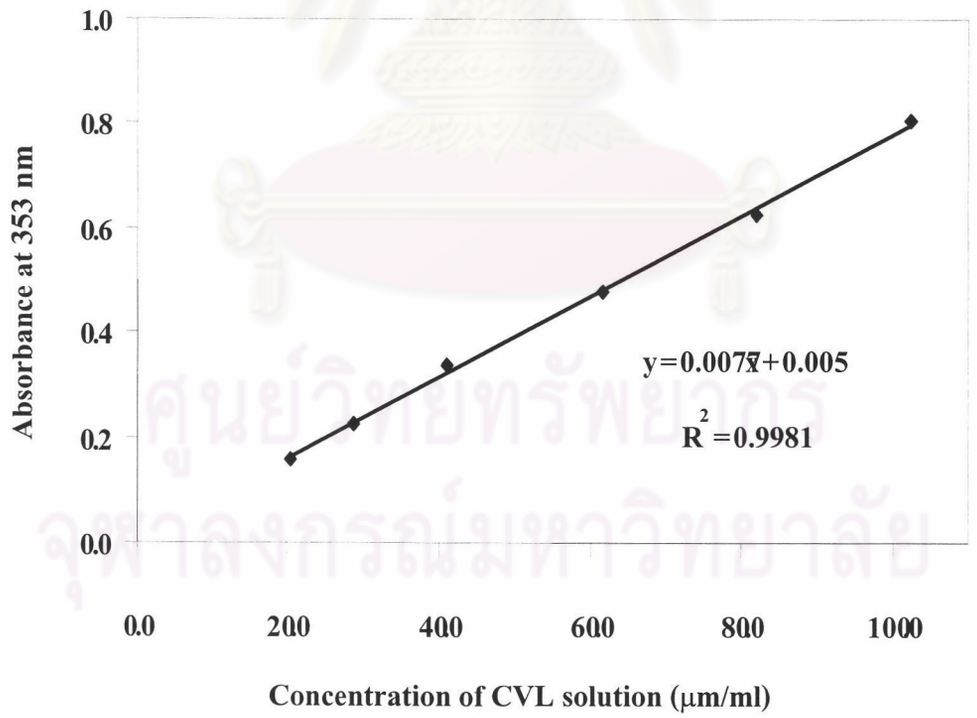

Figure 4.16 Calibration curve of the CVL assayed by UV/Visible spectrophotometry ($r^2 = 0.9981$)

4.5.2 Standard Curve of the Developed CVL

UV/Visible spectrophotometer was used to determine the developed CVL in microcapsules after extraction. In aqueous solution, the developed CVL can absorb visible light at the wavelength range of 609-610 nm. The wavelength used to analyze the developed CVL in this study was 610 nm since it was the λ_{max} of the developed CVL in this medium.

Figure 4.17 shows the absorbance of the developed CVL standard solution at various concentrations. A standard curve was plotted between the developed CVL absorbance at 610 nm and its concentration, and was fitted using a linear regression analysis. The results are presented in Table 4.3 and Figure 4.17. A straight line is obtained with a coefficient of determination (r^2) of 0.9998. The regression equation of this line is

$$y = 0.0059 + 0.2014x \qquad (4.3)$$

where y is the absorbance of the developed CVL and x is the concentration of the developed CVL solution in μg/ml. This equation was used to calculate the amount of CVL remained in the residue of microcapsule powder after extraction by acetone.

4.5.3 Microencapsulation Efficiency

The amount of the CVL was determined from the standard curve. As shown from Table 4.4, the amount of CVL remained in the residue after extraction is negligible.

$$\% \text{ Theoretical content} = \frac{\text{Wt of microcapsules X Wt of CVL x100}}{\text{Wt of core material + Wt of wall material}} \quad (4.4)$$

$$\% \text{ Observed content} = \frac{\text{Assayed amount of CVL X 100}}{\text{Wt of microcapsules}} \quad (4.5)$$

$$\% \text{ Encapsulation efficiency} = \frac{\% \text{ Observed content X 100}}{\% \text{ Theoretical content}} \quad (4.6)$$

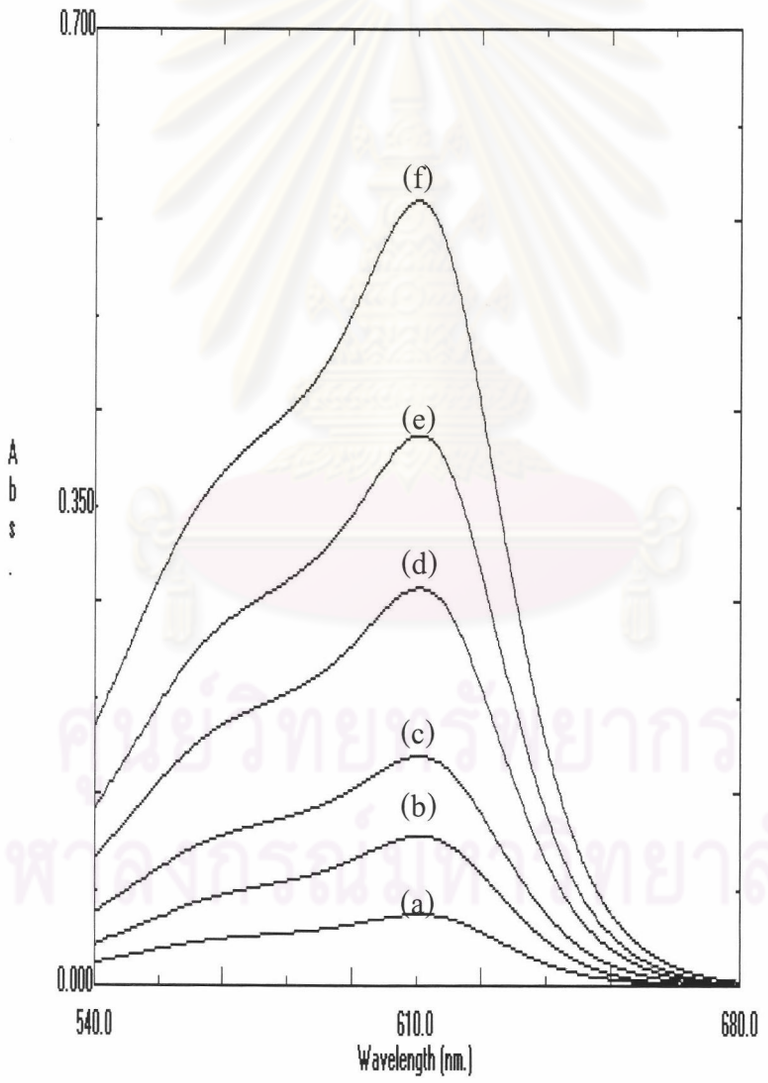

Figure 4.17 Absorbance of standard solutions of the developed CVL at the concentrations of (a) 0.29, (b) 0.58, (c) 0.87, (d) 1.45, (e) 2.02 and (f) 2.89 μg/ml.

Table 4.4 Absorbance of the data of the developed CVL assayed by UV/Visible spectrophotometry.

Standard solution no.	Concentration (μg/ml)	Absorbance at 610 nm.
1	0.289	0.052
2	0.578	0.109
3	0.867	0.167
4	1.445	0.290
5	2.023	0.402
6	2.89	0.574

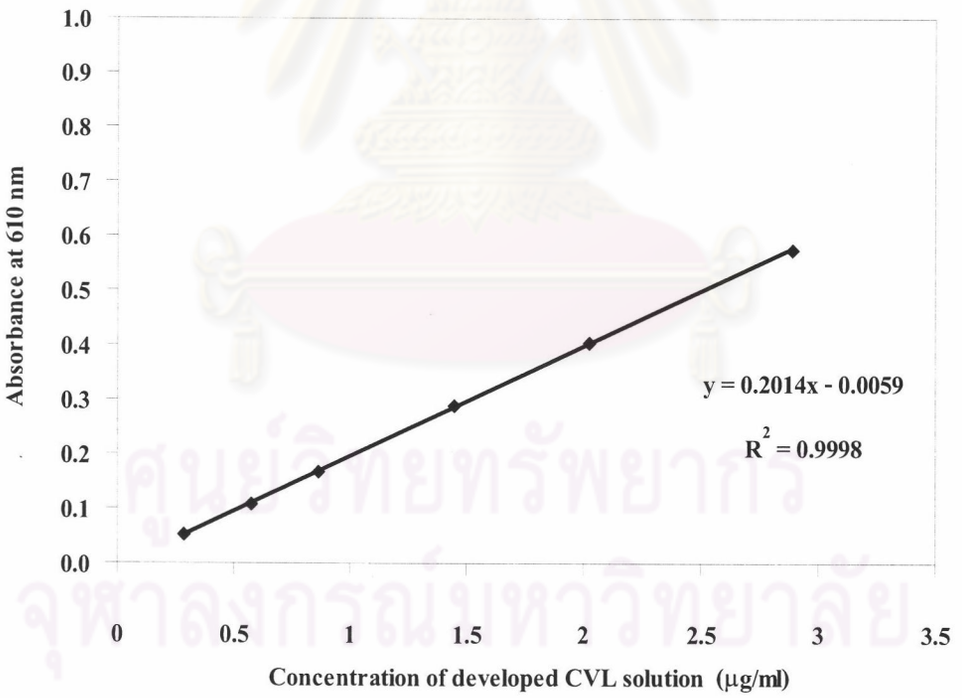

Figure 4.18 Calibration curve of the developed CVL assayed by UV/Visible spectrophotometry ($r^2 = 0.9998$)

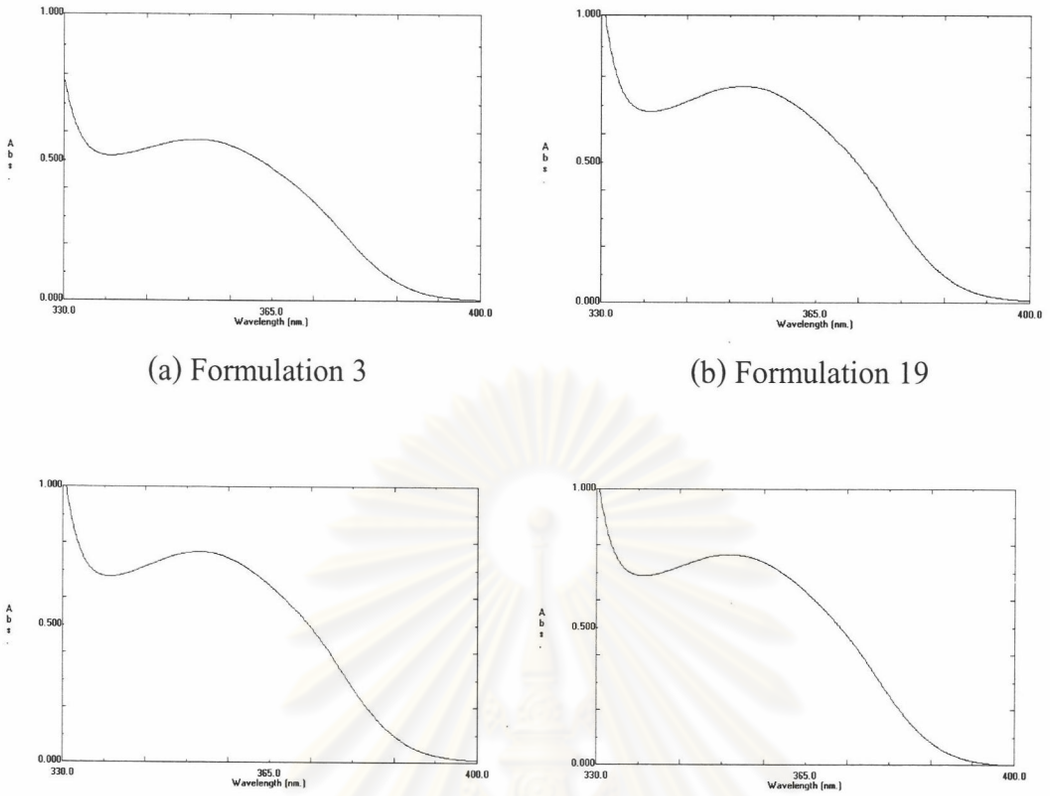

(a) Formulation 3 (b) Formulation 19

(c) Formulation 20 (d) formulation 21

Figure 4.19 Spectra of the CVL containing polyurea microcapsules prepared from 0.06 mole HDI and 0.04 mole MDI and different moles of EDA (a) None, (b) 0.01 mole EDA, (c) 0.02 mole EDA, (c) 0.03 mole EDA.

Table 4.5 Encapsulation efficiency.

Formulation No.	EDA Conc. (mole)	Microcapsule Weight (mg)	CVL content (μg)		Encapsulation Efficiency (%)
			Extraction	Residue	
3	None	302	7389	19.1	45.8
19	0.01	304	9896	21.0	65.5
20	0.02	307	10078	17.3	66.2
21	0.03	308	9857	23.6	64.7

As depicted in Table 4.5, the encapsulation efficiency increased with added EDA at 0.01 mole. Even though increases in the EDA concentration up to 0.02 and 0.03 mole did not influence the encapsulation efficiency of the microencapsules. It seems to relate with the rapid reaction of EDA with diisocyanates, its encapsulation needed less reaction time and the loss of the core material through the wall lessened during the reaction. Therefore, the optimum amount of EDA was 0.01 mole, which can improve encapsulation efficiency of CVL in HDI-MDI based polyurea microcapsules.